Korean J. Chem. Eng., **31**(12), 2237-2244 (2014)
DOI: 10.1007/s11814-014-0179-z

pISSN: 0256-1115
eISSN: 1975-7220

Adsorption of vanadium(V) from acidic solutions by using octylamine functionalized magnetite nanoparticles as a novel adsorbent

Masoome Parijaee*, Mohammad Noaparast*,†, Kamal Saberyan, and Sayyed Ziaadin Shafaie-Tonkaboni***

*Mineral Processing Engineering Department, School of Mining Engineering, University College of Engineering, University of Tehran, Tehran, Iran
**NFCRS, Nuclear Science and Technology Research Institute, P. O. Box 11365-8486, Tehran, Iran
(*Received 15 January 2014 • accepted 27 June 2014*)

Abstract−Adsorption of vanadium(V) from acidic solutions was investigated by using octylamine functionalized magnetite nanoparticles as a novel adsorbent of vanadium. Batch experiments were conducted to determine the effects of initial pH, nanoparticles to octylamine weight ratio, amount of adsorbent, stirring time and initial vanadium(V) concentration in aqueous solution on adsorption efficiency. The adsorption was highly pH dependent, and the optimal pH was 3.2. The weight ratio of magnetite nanoparticles to octylamine was studied in optimum pH, and the best result was 3 : 2. More than 88% of vanadium(V) in solution was removed by 38.4 mg of adsorbent. In kinetics studies, the adsorption equilibrium could be achieved within 10 minutes, and the experimental data were well fitted by the pseudo-second-order model. Comparison of Langmuir and Freundlich isotherm models indicated a better fit of Langmuir model to the adsorption of vanadium(V) and the mono-layer adsorption capacity for vanadium(V) was 25.707 mg g^{-1}.

Keywords: Vanadium (V), Magnetite, Octylamine, Magnetic Nanoparticles, Isotherm Studies

INTRODUCTION

Vanadium, which is found in over 50 different minerals, is the 22nd most abundant element in the earth's crust at a mean concentration of 150 g t^{-1} and with fifth most abundant transition metal has been recognized as a potential pollutant [1]. Never found in its pure form, vanadium originates from primary sources such as ores, concentrates, metallurgical process slag, and petroleum residues. It occurs in combination with various minerals which include carnotite, roscoelite, vanadinite, mottramite and patronite as important sources of the metal [2-4]. The vanadium contents of soils are related to those of the parent rocks from which they are formed and range from 10 to 220 mg kg^{-1}, the highest concentrations being found in shales and clays [5].

Vanadium, due to its tensile strength, hardness, and fatigue resistance, is widely used in industrial processes including the production of special steels, temperature-resistant alloys, glass industry, pigments and paints production, lining arc welding electrodes and as catalyst [3-5].

Vanadium is known as an essential trace element for plants and animals and it is important for biological systems at low concentrations (mg L^{-1}). Indeed, it is essential to cell growth and is known to possess anti-cancer, anti-diabetic, and anti-HIV properties. But vanadium and its many compounds at higher concentrations, depending on the chemical form and exposure level, are toxic to plants, mice, fresh water organisms, and humans and to the whole biosphere. Vanadium is more toxic when inhaled and relatively less when ingested. The oxidation state of vanadium dictates the health hazards upon exposure. Vanadium pentoxide is more toxic than the V (IV) and V (III) oxidation states, and its elemental form [2,3,5].

Vanadium compounds released in large quantities, mainly from fossil fuels combustion and also from various industrial processes, are precipitated on the soil drained by rain and groundwater and may be directly adsorbed by plants [5]. Vanadium compounds are recycled where feasible rather than disposed due to the associated health hazards [2].

Chemical processes are used to treat spent catalysts to recover the vanadium for conversion to oxides and others [6-8]. The general methods developed for the recovery or removal of vanadium ions from aqueous solutions are precipitation [9], ionic exchange [10-12], sorption and solvent extraction [13-15]. Among these, solvent extraction is commonly used for the recovery of vanadium ions because of its high efficiency and the availability of different extractants. Various kinds of extractants for removing and recovering vanadium from aqueous solutions have been reported [4,8,9,13-21]. Among them, amines are famous and effective adsorbents for vanadium due to their selectiveness and high uptake capacity [17].

However, the above-mentioned methods are complex processes that suffer from large secondary wastes, significant chemical additives, solvent losses, complex equipment, and bulky design [22,23]. So, recently, magnetically assisted chemical separation (MACS) processes have been applied for removing heavy metals from aqueous solutions by applying an appropriate magnetic field [22-30]. MACS employs small ferromagnetic particles coated with a selective solvent extractant or ion exchange material [22]. Ferromagnetic nanoparticles, particularly Fe_3O_4 nanoparticles are gaining increasing attention due to their unique magnetic properties and feasibility of preparation, but magnetic nanoparticles easily aggregate because of anisotropic dipolar attraction. Usually, a protection layer is required to ensure chemical stability and improve their dispersibility [31].

†To whom correspondence should be addressed.
E-mail: noparast@ut.ac.ir

To the best of our knowledge, no research efforts have been made at investigation of vanadium removal or recovery by magnetic nanoparticles. In this study the adsorption of vanadium (V) was investigated by octylamine functionalized magnetite nanoparticles (OAF-MNPs) in order to find the optimized conditions of the process.

MATERIALS AND EQUIPMENT

1. Materials

All chemicals including V_2O_5, $FeCl_2 \cdot 4H_2O$, $FeCl_3 \cdot 6H_2O$, NaOH, HCl and Octylamine (by the general structure [R-NH_2] with the total carbon number of 8) with analytical grade were supplied from MERCK Company and were used without any further purification.

2. Equipment and Instrumentation

Vanadium concentration in aqueous solution was determined by inductively coupled plasma optical emission spectrometry (ICP-OES) (Perkin-Elmer 2000 DV model). Synthesized nanoparticles were studied by X-Ray powder diffraction (XRD) measurements (STADI-MP, STOE Company, with monochromatized Cu Kα radiation) and FTIR method (Bruker Vector 22 model) was used for its functional groups investigations in the range of 4,000-400 cm^{-1}. Synthesized nanoparticles were dispersed by ultrasonic cleaner model clean 01. The pH of solution was measured using pH meter model 691 Metrohm.

EXPERIMENTAL

1. Synthesize of Magnetite Nanoparticles

Magnetite nanoparticles were synthesized by normal co-precipitation method [32] by using Fe^{2+}, Fe^{3+} and NaOH, according to reaction (1). Briefly, 25 ml of $FeCl_2 \cdot 4H_2O$ (4.3 mmol) and $FeCl_3 \cdot 6H_2O$ (8.6 mmol) solutions were prepared in 0.6 M HCl and deoxygenized by argon inert gas for 15 minutes. 25 mL of 2 M NaOH was slowly dropped into a three-necked flask containing iron chloride solution under argon gas injection. Final pH was 11.5. The black product was washed several times by distilled water until pH about 7. Finally, it was dried at 50 °C for 24 hours, ground, and then characterized by XRD analysis.

$$Fe^{2+} + 2Fe^{3+} + 8OH^- \rightarrow Fe_3O_4 + 4H_2O \quad (1)$$

2. Preparing of Adsorbent

Magnetite nanoparticles were dispersed in ethanol using an ultrasonic bath for 1 hour. After removing from the bath, the proper amount of octylamine in ethanol was added to it, and was stirred for 8 hours at 500 rpm. The particles were collected by a rare earth magnet (1 tesla) and ethanol was discarded, then they were washed by fresh ethanol and afterwards prepared in certain volume for further experiments.

3. Adsorption of Vanadium (V)

A stock solution of 2,000 mg L^{-1} vanadium (V) was made up by dissolving the proper amount of solid V_2O_5 in 1 molar hydrochloric acid, and it was used for preparing other concentrations of vanadium (V) solutions. Adsorption of vanadium with different concentrations in 19 mL aqueous phase at adjusted pH was carried out by adding 1 mL of adsorbent (certain amount of nanoparticles in distilled water) under mechanical stirring (500 rpm) in a beaker at 25 °C temperature for a given time. After adsorption in defined conditions, the adsorbent was separated by an external magnetic field (1 tesla), and the vanadium concentration in raffinate was measured by ICP-OES. All experiments were run twice, and the adsorption data were the average of obtained results. The amount of adsorbed V (V) was determined using the difference between vanadium concentration in aqueous solution before and after the adsorption. The percentage of vanadium adsorption from aqueous solution was calculated by Eq. (1):

$$\text{Adsorption}\ (\%) = \frac{C_0 - C}{C_0} \times 100 \quad (2)$$

where C_0 and C are initial and final concentrations of vanadium in

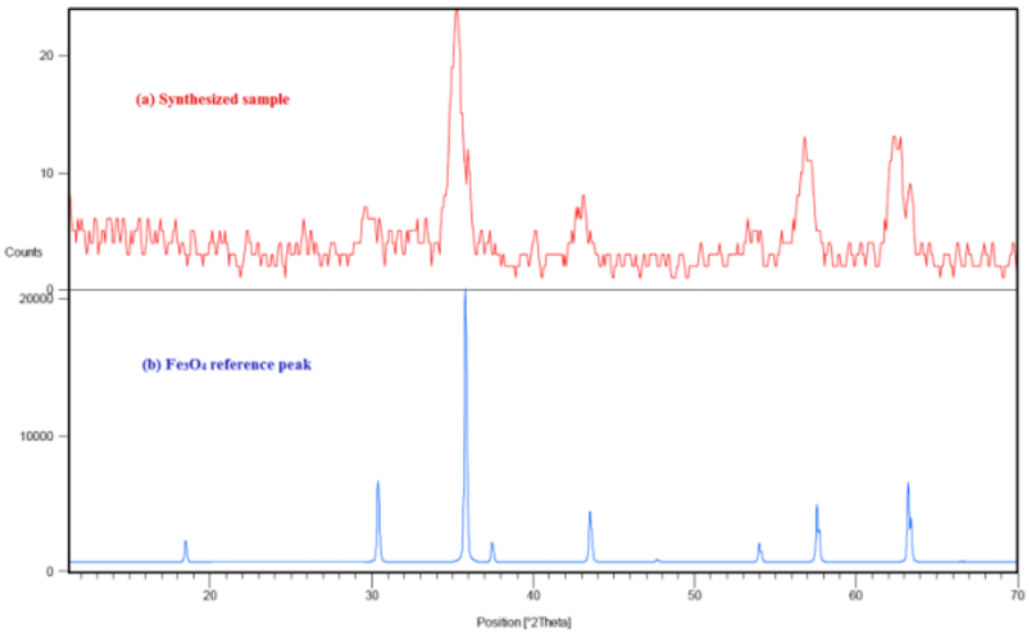

Fig. 1. XRD pattern of (a) synthesized nanoparticles and (b) reference magnetite particles.

the solution (mg L^{-1}), respectively. Adsorption isotherms were studied by experiments performed in 38 mg of adsorbent concentration and optimized conditions. The amount of metal adsorbed q_e (mg g^{-1}) was determined by using the Eq. (2):

$$q_e = \frac{(C_0 - C_e)V}{m} \quad (3)$$

where C_0 and C_e represent the initial and equilibrium metal ion concentrations (mg L^{-1}), respectively; V is the volume of the metal ion solution (mL), and m is the amount of adsorbent (mg).

RESULTS AND DISCUSSION

1. Characterization of Nanoparticles and Adsorbent

The X-ray diffraction pattern for synthesized nanoparticles and reference peak for magnetite are shown in Fig. 1. Comparison of the two peaks confirms that synthesized nanoparticles were magnetite. The size of these nanoparticles was estimated by Scherer equation equal to 15 nm [33]. Magnetite nanoparticles synthesized by co-precipitation method in this size range have superparamagnetic behavior [34,35].

The functional groups of amine-modified magnetite nanoparticles were identified using FTIR (Fig. 2). The bands centered around 3,440 cm^{-1} and 1,635 cm^{-1} are, respectively, assigned to the stretching and deforming vibrations of O-H group on the surface of nanoparticles [31,36]. The peak at 570 cm^{-1}, corresponds to the Fe-O vibration of Fe_3O_4 [31]. A band in the region of 2,930 cm^{-1} was ascribed to asymmetric stretching of the C-H_2 groups. Two weak bands around 2,930 cm^{-1} were attributed to symmetric stretching of C-H_2 and asymmetric stretching of C-H_3 [37].

One of the characteristics of primary and secondary amines is a sharp peak around 3,440 cm^{-1} representing the stretching vibration of N-H groups equal to number of N-H bond, but the broad stretching band corresponding to O-H stretching vibration overlapped with this peak. Furthermore, a peak around 1,650 cm^{-1} bending-scissoring vibration of N-H_2 that is only observed for primary amines in 1,630 cm^{-1} overlapped by O-H deforming vibration. A band at 1,053 cm^{-1} is assigned to C-N stretching vibrations [37]. The results indicated that amino-group has been grafted onto the Fe_3O_4 nanoparticles.

The OAFMNPs particles in aqueous solution were black emulsion with stability even after one month. They were easily separated from solution in a few seconds, under an external magnetic field. Observations demonstrated easy and fast separation of the OAFMNPs after the adsorption experiments.

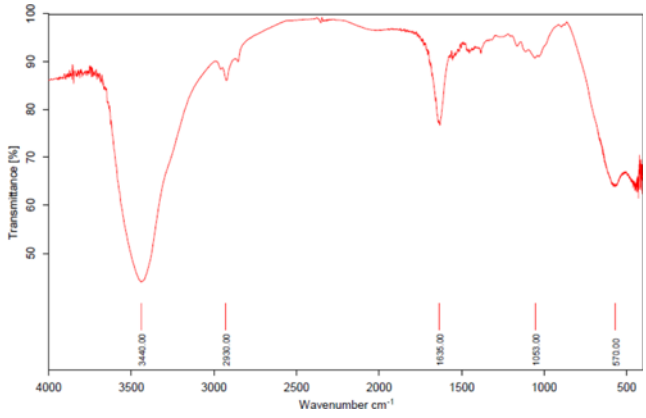

Fig. 2. FT-IR spectrum of OAFMNPs.

2. Vanadium Solution Chemistry

Vanadium behavior in the adsorption process is extremely affected by the predominant species in aqueous phase, so considering its solution chemistry is an essential impact. Vanadium as a transition metal has several oxidation states from −1 to +5, but it is most commonly found in the +4 and +5 states as tetravalent vanadyl (VO^{2+}) and pentavalent vanadate (HVO_4^{2-}, VO_3^- and/or $H_2VO_4^-$) species, respectively, in the monomeric and polymeric forms [3,5,7,38,39]. The multiple oxidation states, ready hydrolysis and polymerization confer a level of complexity to the chemistry of vanadium well above that of many metals [5].

Oxidation states of vanadium depend on vanadium and ligand concentrations in solution, pH and solution potential (Eh) [7,38,39]. In leach liquors from the processing of spent catalysts, ores and residues, the predominant species in acidic medium are vanadium (IV) and (V) and in alkaline medium is vanadium (V) [3,5,7,13]. Though the conditions are strongly reducing, vanadium may also exist as trivalent V (III) and divalent V (II) ions [3].

An interesting feature of vanadium is the phenomenon of polymerization depending on pH values and concentrations [7,38,39]. Figs. 3 and 4 are the species of vanadium (V) existing in an aqueous solution under different pH and concentrations [39,40]. Fig. 3 represents that the cationic vanadium species are predominant at pH<2 [3,5,7,38,39].

Vanadium (IV), as the vanadyl cation VO^{2+}, may be present in reducing environment. It is stable in acidic solution below of pH=2, but is oxidized to the pentavalent state by atmospheric oxygen at higher pH values [3,5].

Polynuclear anionic species such as decavanadate $V_{10}O_{28}^{6-}$ or metavanadate $V_4O_{12}^{4-}$ are predominant in the pH range of 2-9, which are partially protonated according to the pH value, while mononuclear anionic species dominate at pH>9 [7,38-40]. In the acid leach solution of stone coal containing 2-3 g L^{-1} V_2O_5 at pH=2-4, vanadium is mostly in the forms of $V_{10}O_{28}^{6-}$, $HV_{10}O_{28}^{5-}$ and $H_2V_{10}O_{28}^{4-}$ [39]. Vari-

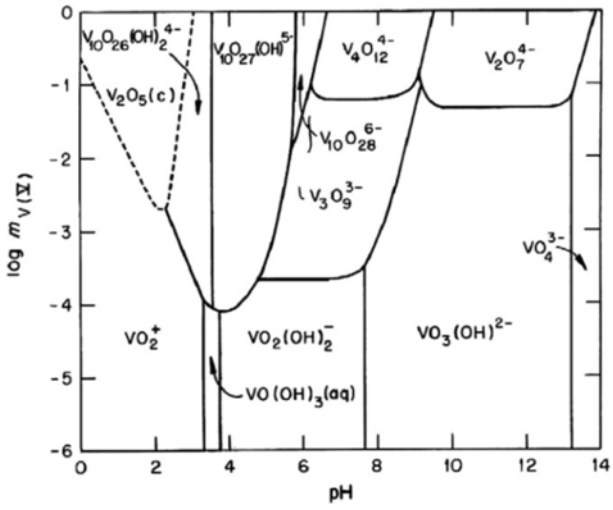

Fig. 3. Equilibrium predominance diagram for V (V)-OH- species as a function of concentration and pH [39].

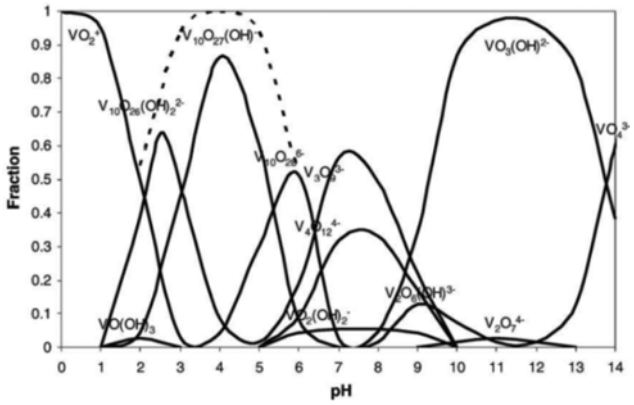

Fig. 4. The distribution of vanadium species in water as a function of pH with a total VO_2^+ concentration of 14.33 mM. The dashed line represents the sum of the distribution percentages of the decavanadates [40].

Table 1. Effect of pH on the formations of predominant species of Vanadium [41]

pH	Vanadium species
>13	VO_4^{3-}
9	$V_2O_7^{4-}$
8.5	VO_3^-
6	$V_3O_9^{3-}$
2	$V_{10}O_{28}^{6-}$
<2	VO_2^+

ous isopolyanions exist in dynamic equilibrium and the predominant species formed at different pH are shown in Table 1 [41].

3. Effect of pH

The solution pH is one of the most important factors in controlling the adsorption of vanadium species by a given adsorbent. As mentioned in section 4-2, depending on the pH and vanadium concentrations, several monomeric and polymeric tetravalent and pentavalent vanadium species can also be present in aqueous solutions. Based on this, among the investigated parameters, priority

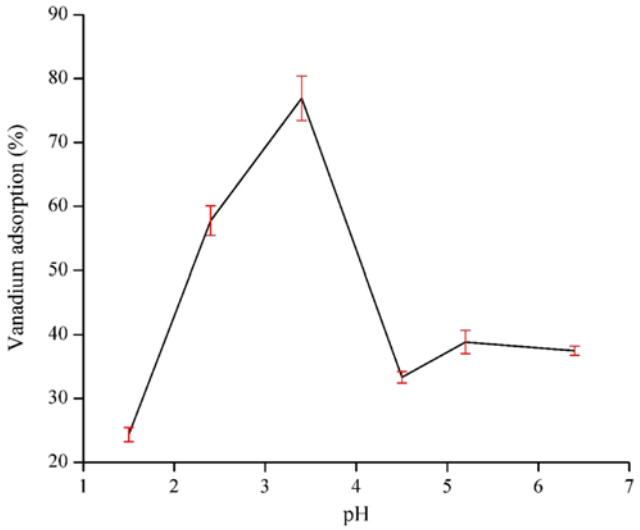

Fig. 5. Effect of pH on vanadium adsorption (30 minutes adsorption time, NPs/OA=4 : 1, 20.0 mL solution volume).

was given to illuminating the effect of pH on vanadium uptake by the adsorbent. This test was performed by adding 1 mL of adsorbent (with magnetite nanoparticles (NPs) to octylamine (OA) weight ratio equal to 4 : 1 in 10 g L^{-1} adsorbent concentration) to 19 mL of vanadium solution with the concentration of about 10 mg L^{-1} in a beaker and adsorption was carried out at 30 minutes in temperature of 25 °C. The results of V (V) adsorption by OAFMNPs as a function of pH are presented in Fig. 5. The highest adsorption of vanadium was at pH 3.2 equal to 77%. The lowest adsorption occurred in pH about 1.5 because of cationic species formation of vanadium according to Fig. 5. This figure shows that cationic species of vanadium comes to lowest amount in pH about 3.2, and since predominant vanadium species is decavanadate, the adsorption of vanadium increases. Although this species predominates till neutral pH, decreasing of H^+ concentration affects protonation of adsorbent. Therefore, the capability of adsorbent for extracting of anionic decavanadate and metavanadate from aqueous solution is reduced ex-

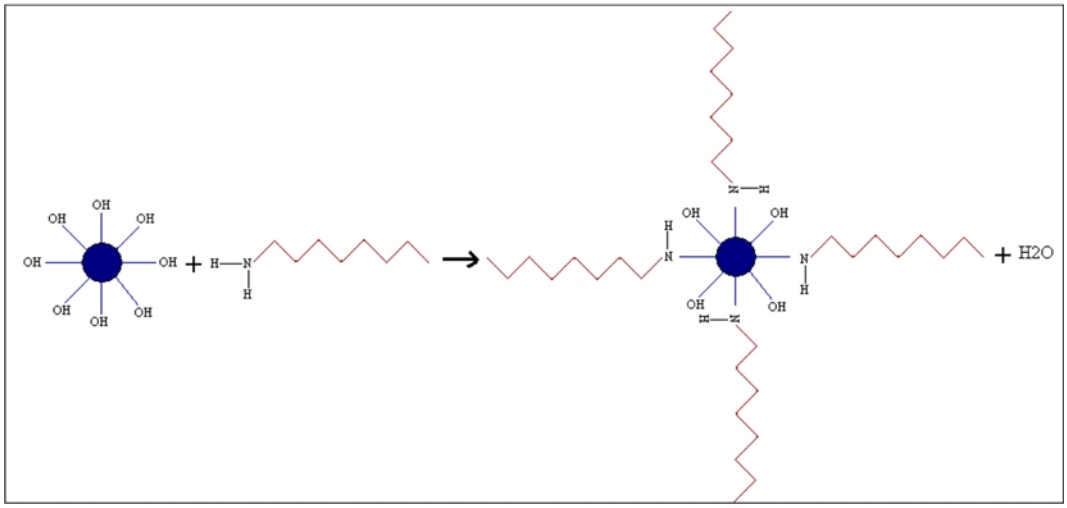

Fig. 6. Schematic of OAFMNPs.

tremely. Additionally, the amount of decavanadate rather metavanadate decreases and impacts on the adsorption percent. The results from the references and the present study indicate the importance of pH adjustment prior to other adsorption parameters. Consequently, a solution pH of 3.2 can be used for the better adsorption of vanadium (V).

3-1. Adsorption Mechanism

Functional groups of -OH, -SH and -NH_2 are used as coating agents for magnetic core due to interaction with this core [42]. Reaction process between primary amine such as octylamine and magnetite nanoparticles can also be of this type (Fig. 6) [43]. This interaction can be written as reaction (2):

$$Fe_3O_4-(OH)_x+y(R-NH_2)\rightarrow Fe_3O_4-(OH)_{x-y}y(R-NH)+yH_2O \quad (4)$$

So $Fe_3O_4-(OH)_{x-y}y(R-NH)$ acts as adsorption agent which can be simplified and assumed as $(Fe_3O_4)-(R-NH)$. The adsorbent after protonation in acidic media is as reaction (3):

$$(Fe_3O_4)-(R-NH)+HCl\rightarrow(Fe_3O_4)-(RNH_2)^+\cdot Cl^- \quad (5)$$

Mechanism of vanadium adsorption in acidic solutions with pH above 2 in which decavanadate species are predominant are considered as reactions (4) to (6):

$$(Fe_3O_4)-(RNH_2)^+\cdot Cl^-+(H_2V_{10}O_{28})^{4-} \rightarrow(Fe_3O_4)-(RNH_2)^+\cdot(H_2V_{10}O_{28})^{4-}+Cl^- \quad (6)$$

$$(Fe_3O_4)-(RNH_2)^+\cdot Cl^-+(HV_{10}O_{28})^{5-} \rightarrow(Fe_3O_4)-(RNH_2)^+\cdot(HV_{10}O_{28})^{5-}+Cl^- \quad (7)$$

$$(Fe_3O_4)-(RNH_2)^+\cdot Cl^-+(V_{10}O_{28})^{6-} \rightarrow(Fe_3O_4)-(RNH_2)^+\cdot(V_{10}O_{28})^{6-}+Cl^- \quad (8)$$

4. Effect of Nanoparticles to Octylamine Weight Ratio

The weight ratio of magnetite nanoparticles to octylamine (NPs/OA) was varied as 3 : 1, 3 : 1.5, 3 : 2, 3 : 3 and 3 : 4 in NPs concentration of 3.8 g L^{-1} to investigate the optimum ratio of NPs/OA. Fig. 7 shows the results of this experiment at pH=3.2. The maximum adsorption of % 48.4 was achieved at 3 : 2 of weight ratio.

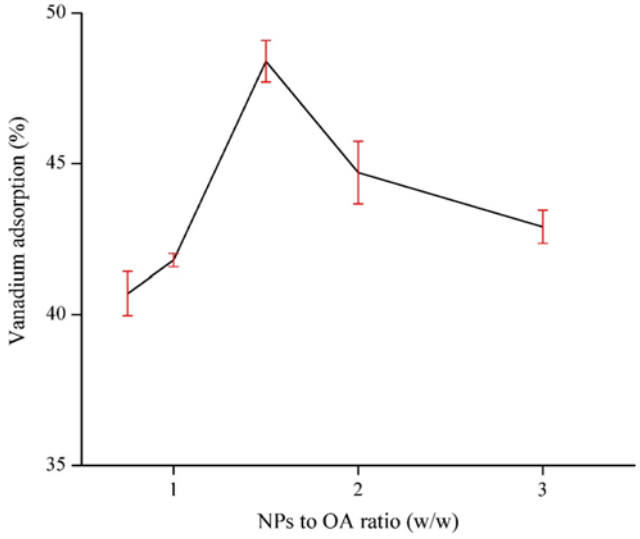

Fig. 7. Effect of NPs to OA weight ratio (NPs concentration=3.8 g L^{-1}) in 20 mL solution and pH of 3.2.

Higher adsorption in Fig. 5 rather than Fig. 7 is due to the higher amount of adsorbent in the former; the amount of nanoparticles in the section 4-3 was 8 mg while in this experiment it was 3.8 mg.

5. Effect of Adsorbent Amount

The optimum amount of the adsorbent for maximum adsorption was determined by varying the OAFMNPs content from 6.4 to 44.8 mg in 1 mL distilled water while keeping the other parameters constant (19.0 mL of 10 mg L^{-1} V (V) solution, pH of 3.2, NPs to OA weight ratio of 3 : 2, reaction temperature of 25 °C). The adsorption percentage of V (V) from solution clearly increases with the increase in OAFMNPs concentration and remains almost constant at about 32 mg with more than 87% adsorption (Fig. 8). The increase in adsorption with an increase in amount of adsorbent would be attributed to the availability of larger surface area and more adsorption sites. With increasing OAFMNPs content, the available sites on magnetic nanoparticles surfaces increase and provide more adsorption sites to adsorb metal ions, and thereby result in increasing of vanadium ion adsorption. From the economical point of view and for guaranteeing quantitative adsorption of V (V), the 38.4 mg adsorbent with 88.7% adsorption was selected as the optimum amount.

6. Effect of Shaking Time and Adsorption Kinetics

The equilibration time between V (V) and the adsorbent was determined by changing the adsorption time between 1-60 minutes while

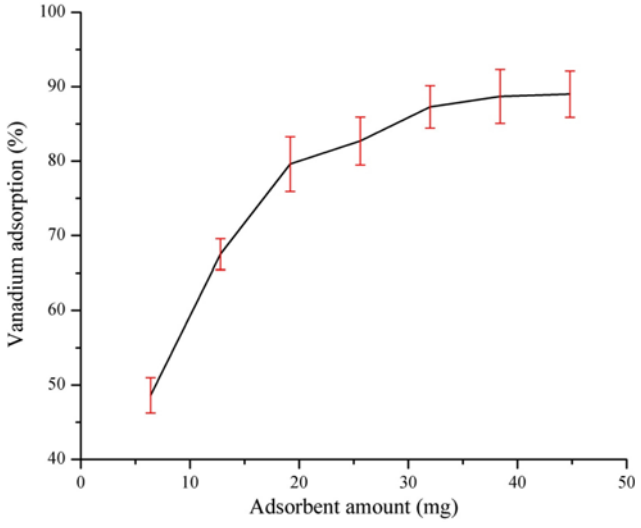

Fig. 8. Effect of adsorbent amount on vanadium adsorption (solution pH of 3.2, 30 minutes adsorption time, NPs/OA=3 : 2, 20.0 mL solution volume).

Table 2. Adsorption of V (V) from solution by OAFMNPs in different contact times

Time (min)	V (V) adsorption (%)	Relative standard error (%)
1	80.4	3.99
5	80.4	4.27
10	84.3	3.26
15	83.3	4.71
30	85.3	4.42
45	84.3	2.68
60	85.3	3.45

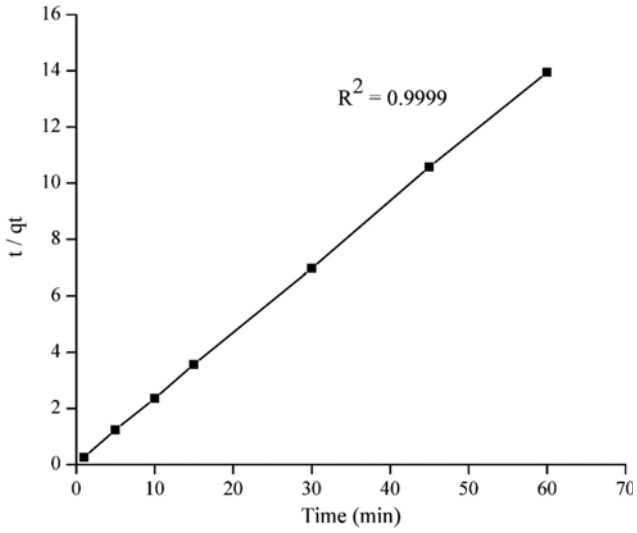

Fig. 9. Kinetics model of vanadium separation.

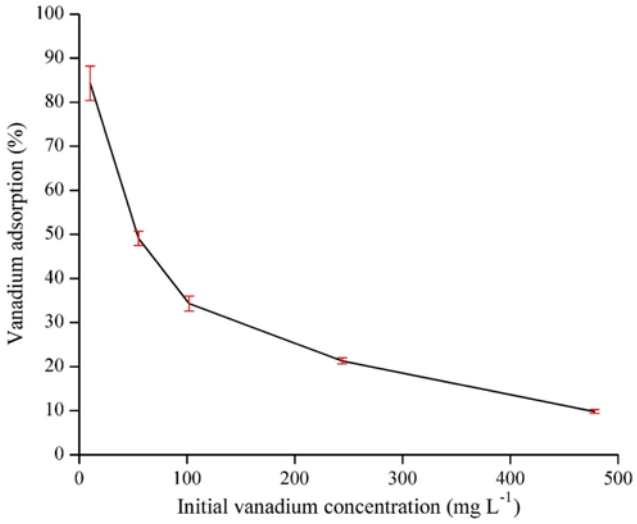

Fig. 10. Effect of initial V (V) concentration on the adsorption by OAFMNPs (38.4 mg adsorbent, 10 minutes adsorption time, solution pH of 3.2, 20.0 mL solution volume).

keeping the other parameters constant (38.4 mg adsorbent, 19 mL of 10 mg L^{-1} V(V) solution, pH of 3.2, NPs to OA ratio of 3 : 2, reaction temperature of 25 °C). The results of V (V) separation from solution by OAFMNPs at different contact times are shown in Table 2. The adsorption capacity of V (V) onto OAFMNPs slightly increases with an increase of contact time, and it remains almost constant after 10 minutes (84.3% adsorption). So a stirring time of 10 minutes was used to quantitative adsorption of vanadium (V).

The adsorption kinetics of vanadium ions by OAFMNPs were analyzed on the basis of the pseudo-second order kinetic model, which is expressed as Eq. (3) [44]:

$$\frac{t}{q_t} = \frac{1}{kq_e^2} + \frac{t}{q_e} \quad (9)$$

where, t (min) is the contact time, q_t and q_e (mg g^{-1}) are the amount of vanadium adsorbed at an arbitrary time t and at equilibrium time, respectively, and k is the rate constant of pseudo-second-order adsorption (g mg^{-1} min^{-1}).

Fig. 9 shows that the pseudo-second-order equation fits well with the experimental data, and the correlation coefficient of linear plot obtained for pseudo-second-order equation is 0.9999. Furthermore, the adsorption capacities calculated by the pseudo-second-order model (q_e cal=4.30 mg g^{-1}) are close to that determined by experiment (q_e exp=4.25 mg g^{-1}). Thus, it would be postulated that the pseudo-second-order kinetic model is better to fit the experimental data and the process may be chemical process.

7. Effect of Initial Vanadium Ion Concentration in Aqueous Phase

The extent of removal of metals from aqueous solutions depends strongly on the initial concentration of the metal [3]. The adsorption percentage of V (V) by OAFMNPs at various initial concentrations of vanadium (10.2, 55, 102, 244 and 478 mg L^{-1}) was studied under the optimum conditions: 38.4 mg sorbent, 19.0 mL V (V) solution, pH of 3.2, reaction temperature of 25 °C. From the obtained results in Fig. 10, the adsorption percentages decrease when initial concentration of vanadium increases. The adsorption is particularly dependent on initial vanadium ion concentration. At low concentration values, metals are adsorbed by specific adsorption sites, while with increasing metal concentration the specific adsorption sites are saturated [31]. Therefore, decreasing the adsorption is due to exceeding the maximum sorption capacity of the sorbent. However, this deficiency can be overcome with the use of higher amounts of OAFMNPs.

7-1. Adsorption Isotherms

The equilibrium adsorption isotherm experiments were performed by plotting metal ions adsorbed (q_e) against the equilibrium concentration of vanadium ions (C_e) in solution (Fig. 11).

Langmuir and Freundlich isotherms equations have been tested for vanadium adsorption by OAFMNPs. The Langmuir adsorption model can be expressed as Eq. (4) [45]:

$$\frac{C_e}{q_e} = \frac{1}{q_L K_L} + \frac{1}{q_L} C_e \quad (10)$$

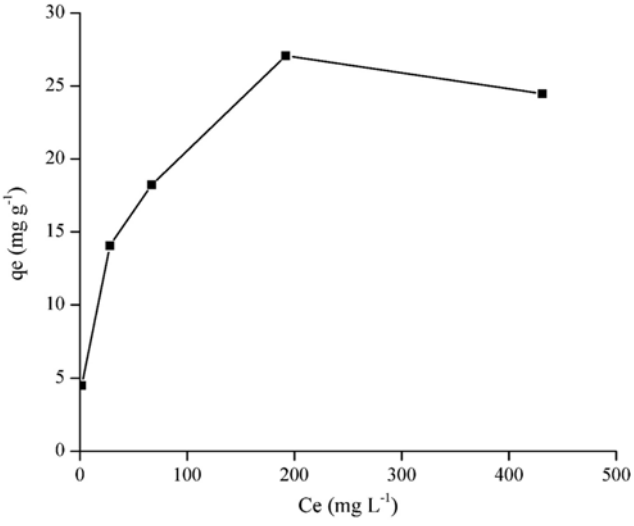

Fig. 11. Adsorption isotherm of V (V) (38.4 mg adsorbent, 10 minutes adsorption time, solution pH of 3.2, 20.0 mL solution volume).

where K_L is the Langmuir adsorption constant (L mg^{-1}) and q_L is the mono-layer adsorption capacity of adsorbent (mg g^{-1}). $1/q_L$ and $1/(q_L K_L)$ in Eq. (4) can be determined by slope and intercepts of the linear plot of C_e/q_e versus C_e, respectively.

The Freundlich model can be expressed as Eq. (5) [45]:

$$\log q_e = \log K_F + \frac{1}{n}\log C_e \tag{11}$$

where K_F and n are the Freundlich adsorption constants. A plot of log q_e versus log C_e gives a straight line of slope 1/n and intercepts log K_F.

Langmuir and Freundlich isotherms models are plotted in Figs. 12 and 13, respectively. Constants of the Langmuir and Freundlich model and the values of the correlation coefficients are shown in Table 3. It can be seen from the correlation coefficients that Langmuir model fits the data better than Freundlich model. The mono-layer adsorption capacity for vanadium ions by OAFMNPs is 25.707 mg g^{-1}.

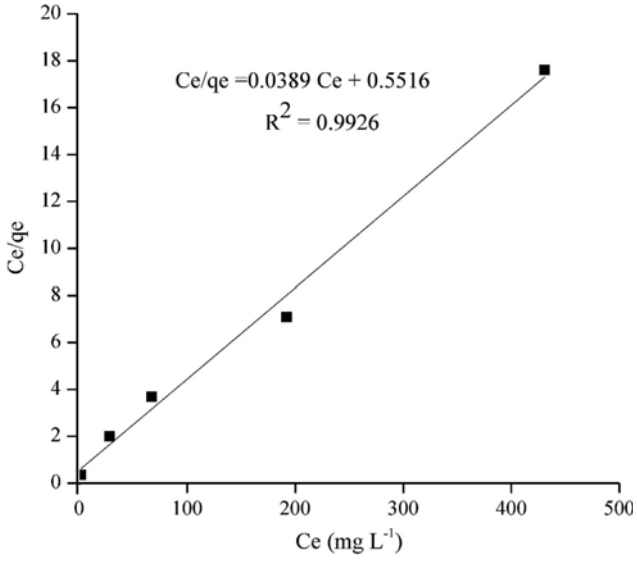

Fig. 12. Langmuir isotherm model (38.4 mg adsorbent, 10 minutes adsorption time, solution pH of 3.2, 20.0 mL solution volume).

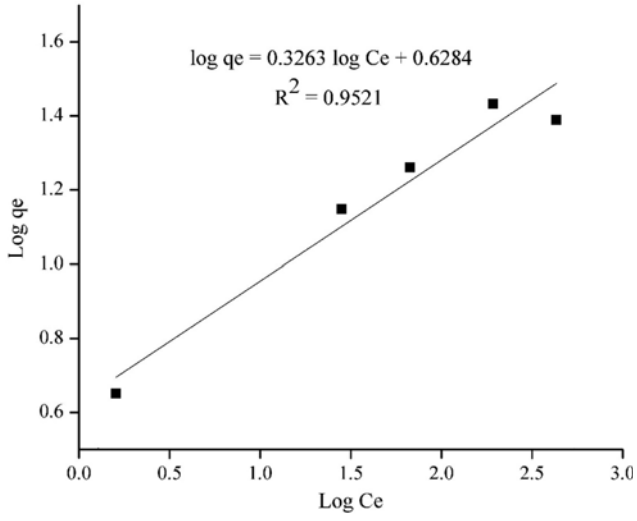

Fig. 13. Freundlich isotherm model (38.4 mg adsorbent, 10 minutes adsorption time, solution pH of 3.2, 20.0 mL solution volume).

Table 3. Langmuir and Freundlich constants for vanadium adsorption by OAFMNPs

Langmuir model			Freundlich model		
q_L	K_L	R^2	n	K_F	R^2
25.707	0.0705	0.9926	3.065	4.250	0.9521

Favorability of vanadium adsorption by OAFMNPs can be obtained by using a separation factor R_L as follows [42]:

$$R_L = \frac{1}{1 + K_L C_{max}} \tag{12}$$

where C_{max} is the highest metal concentration in solution (mg L^{-1}). If R_L is considerably less than 1.0, the adsorption is considered to be favorable. In present study R_L is 0.029 for C_{max} equal to 478 mg L^{-1}. So adsorption of vanadium on OAFMNPs can be considered to be favorable.

CONCLUSION

Octylamine functionalized magnetite nanoparticles (OAFMNPs) were applied as the novel adsorbent of vanadium (V) from acidic solution in this study. Effects of initial pH, nanoparticles to octylamine weight ratio, amount of adsorbent, stirring time and initial V (V) concentrations in aqueous solutions on vanadium adsorption efficiency were investigated using magnetically assisted chemical separation, MACS, method. The results indicated that anionic species of vanadate could be absorbed by these modified nanoparticles and adsorption was highly pH dependent. At optimal pH of 3.2, the weight ratio of magnetite nanoparticle to octylamine was studied, with the best result for 3 : 2. Highest removal of V (V) obtained in adsorbent amount of about 38 mg after 30 minutes with more that 88% of V (V) in solution. Stirring time studies showed that kinetics of adsorption was very rapid so that vanadium in solution could reach equilibrium within 10 minutes. Adsorption of vanadium was decreased by increasing the initial vanadium concentration due to exceeding the maximum sorption capacity of adsorbent in higher vanadium concentration. The isotherm data have been analyzed using Langmuir and Freundlich isotherm models. Comparison of the values of the correlation coefficients for Langmuir and Freundlich isotherms indicated that the mono-layer Longmuir model provides better correlation for adsorption of vanadium and the mono-layer adsorption capacity for vanadium ions removal by OAFMNPs is 25.707 mg g^{-1}. The present study suggests that OAFMNPs would be employed as a potential adsorbent for vanadium adsorption, and also could provide a simple and fast separation method for removal of V (V) metal ion from aqueous solution.

NOMENCLATURE

C : final concentrations of metal in the solution [mg L^{-1}]
C_0 : initial metal ion concentrations [mg L^{-1}]

C_e : equilibrium metal ion concentrations [mg L^{-1}]
C_{max} : the highest metal concentration in solution [mg L^{-1}]
K : the rate constant of pseudo-second-order kinetics model
K_F : Freundlich adsorption constants
K_L : Langmuir adsorption constant [L mg^{-1}]
M : amount of adsorbent [mg]
MACS : magnetically assisted chemical separation
N : Freundlich adsorption constants
NPs : nanoparticles
OA : octylamine
OAFMNPs : octylamine functionalized magnetite nanoparticles
q_e : amount of metal adsorbed [mgg^{-1}]
q_L : mono-layer adsorption capacity of adsorbent [mg g^{-1}]
R_L : separation factor
T : time [min]
V : volume of the metal ion solution [mL]

REFERENCES

1. F. Habashi, In *Proceedings of the International Symposium on Vanadium*, M. F. Tanner, P. A. Riveros, J. E. Dutrizac, M. Gattrell and L. Perron, Eds., Conference of Metallurgists, Montreal, Canada (2002).
2. R. R. Moskalyk and A. M. Alfantazi, *Miner. Eng.*, **16**, 793 (2003).
3. A. Erdem, T. Shahwan, A. Çağır andA. E. Eroğlu, *Chem. Eng. J.*, **174**, 76 (2011).
4. D. He, Q. Feng, G. Zhang, L. Ou and Y. Lu, *Miner. Eng.*, **20**, 1184 (2007).
5. K. Pyrzyáska and T. Wierzbicki, *Talanta*, **64**, 823 (2004).
6. Y. Shao, Q. Feng, Y. Chen, L. Ou, G. Zhang and Y. Lu, *Hydrometallurgy*, **96**, 166 (2009).
7. L. Zeng and C. Y. Cheng, *Hydrometallurgy*, **98**, 10 (2009).
8. L. Zeng and C. Y. Cheng, *Hydrometallurgy*, **101**, 141 (2010).
9. A. Chagnes, M. Rager, B. Courtaud, J. Thiry and G. Cote, *Hydrometallurgy*, **104**, 20 (2010).
10. L. Zeng, Q. Li and L. Xiao, *Hydrometallurgy*, **97**, 194 (2009).
11. X. Wang, M. Wang, L. Shi, J. Hu and P. Qiao, *Hydrometallurgy*, **104**, 317 (2010).
12. J. Hu, X. Wang, L. Xiao, S. Song and B. Zhang, *Hydrometallurgy*, **95**, 203 (2009).
13. Y. A. El-Nadi, N. S. Awwad and A. A. Nayl, *Int. J. Miner. Process.*, **90**, 115 (2009).
14. L. J. Lozano and C. Godınez, *Miner. Eng.*, **16**, 291 (2003).
15. T. Cosar and R. Ziyadanogullari, *Turk J. Chem.*, **22**, 379 (1998).
16. Y. Bal, K.-E. Bal, G. Cote and A. Lallam, *Hydrometallurgy*, **75**, 123 (2004).
17. P. Ning, H. Cao, C. Liu, Y. Li and Y. Zhang, *Hydrometallurgy*, **97**, 131 (2009).
18. A. Chagnes, C. Fosse, B. Courtaud, J. Thiry and G. Cote, *Hydrometallurgy*, **105**, 328 (2011).
19. D. Zhi-gan, W. Chang, F. Gang, L. Min-ting, L. Cun-xiong and L. Xing-bin, *Transactions of Nonferrous Metals Society of China*, **20**, 118 (2010).
20. R. Navarro, J. Guzman, I. Saucedo, J. Revilla and E. Guibal, *Waste Manage.*, **27**, 425 (2007).
21. X. Li, C. Wei, Z. Deng, M. Li, C. Li and G. Fan, *Hydrometallurgy*, **105**, 359 (2011).
22. M. D. Kaminski and L. Nunez, *J. Magn. Magn. Mater.*, **194**, 31 (1999).
23. B. S. Shaibu, M. L. P.Reddy, A. Bhattacharyya and V. K. Manchanda, *J. Magn. Magn. Mater.*, **301**, 312 (2006).
24. L. M. Rossi, L. L. R. Vono, F. P. Silva, P. K. Kiyohara, E. L. Duarte and J. R. Matos, *Appl. Catal. A: Gen.*, **330**, 139 (2007).
25. A. F. Ngomsik, A. Bee, J. M. Siaugue, D. Talbot, V. Cabuil and G. Cote, *J. Hazard. Mater.*, **166**(2-3), 1043 (2009).
26. A. A. Atia, A. M. Donia and A. M. Yousif, *Sep. Purif. Technol.*, **61**, 348 (2008).
27. C. Yi-Fu, C. Tsai, C. Chou and F. Yang, *ISEIS, Environmental Informatics Archives*, **4**, 218 (2006).
28. L. L. Vatta, R. D. Sanderson and K. R. Koch, *IUPAC, Pure Appl. Chem.*, **78**(9), 1793 (2006).
29. L. Nunez and M. D. Kaminski, *J. Magn. Magn. Mater.*, **194**, 102 (1999).
30. S. E. Matthew, P. Parzuchowski, A. Garcia-Carrera, C. Grüttner, J. F. Dozol and V. Böhmer, *Chem. Commun.*, 417 (2001).
31. F. L. Fan, Z. Qin, J. Bai, W. D. Rong, F. Y. Fan, W. Tian, X. L. Wu, Y. Wang and L. Zhao, *J. Environ. Radioact.*, **106**, 40 (2012).
32. Z. Yuanbi, Q. Zumin and H. Jiaying, *Chin. J. Chem. Eng.*, **16**(3), 451 (2008).
33. B. D. Cullity and S. R. Stock, *Elements of X-ray diffraction*, Prentice Hall, Upper Saddle River (2001).
34. P. E. G. Casillas, C. A. R. Gonzalez and C. A. M. Perez, In *Infrared Spectroscopy- Material Science, Engineering and Technology*, T. Theophanides, Ed., InTech (2012).
35. M. A.Verges, R. Costo, A. G. Roca, J. F. Marco, G. F. Goya, C. J. Serna and M. P. Morales, *J. Phys. D: Appl. Phys.*, **41**, 1 (2008).
36. H. Hu, Z. Wang and L. Pan, *J. Alloy Comp.*, **492**, 656 (2010).
37. B. Stuart, *Infrared spectroscopy: Fundamentals and applications*, John Wiley & Sons, Ltd. (2004).
38. L. Luo, T. Miyazaki, A. Shibayama, W. Yen and T. Fujita, *Miner. Eng.*, **16**, 665 (2003).
39. L. Zeng, Q. Li, L. Xiao and Q. Zhang, *Hydrometallurgy*, **105**, 176 (2010).
40. M. A. Olazabal, M. M. Orive, L. A. Fernandez and J. M. Madariaga, *Solvent Extr. Ion Exch.*, **10**(4), 623 (1992).
41. S. K. Tangri, A. K. Suri and C. K. Gupta, *Transactions of the Indian Institute of Metals*, **51**(1), 27 (1998).
42. S. Laurent, D. Forge, M. Port, A. Roch, C. Robic, L. V. Elst and R. N. Muller, *Chem. Rev.*, **108**(6), 2064 (2008).
43. T. Mousavand, S. Takami, M. Umetsu, S. Ohara and T. Adschiri, *J. Mater. Sci.*, **41**, 1445 (2006).
44. Y. S. Ho, *J. Hazard. Mater.*, **B136**, 681 (2006).
45. S. Liang, X. Guo, N. Feng and O. Tian, *J. Hazard. Mater.*, **174**, 756 (2010).